

The Design of Planar Serial Manipulators with Decoupled Dynamics Taking into Account the Changing Payload

Jiali Xu^{1*}, Vigen Arakelian^{1,2*} and Jean-Paul Le Baron¹

¹ Mecaproce, INSA of Rennes, Rennes, France

² Institut de Recherche en Communication et Cybernétique de Nantes, Nantes, France

***Corresponding author:** Vigen Arakelian, Institut de Recherche en Communications et Cybernétique de Nantes (IRCCyN) and the Mecaproce of the INSA of Rennes, 20 av. des Buttes de Coesmes, CS 70839, F-35708 Rennes, France; Email: Vigen.Arakelyan@irccyn.ec-nantes.fr; vigen.arakelyan@insa-rennes.fr.

Jiali Xu, Mecaproce of the INSA of Rennes, 20 Avenue des Buttes de Coesmes, CS 70839, F-35708 Rennes, France; Tel: +33(0)223238492; Fax: +33(0)223238726; Email: Jiali.Xu@insa-rennes.fr.

Article Type: Research, **Submission Date:** 18 October 2016, **Accepted Date:** 17 November 2016, **Published Date:** 19 December 2016.

Citation: Jiali Xu, Vigen Arakelian and Jean-Paul Le Baron (2016) The Design of Planar Serial Manipulators with Decoupled Dynamics Taking into Account the Changing Payload. J Robot Mech Eng Resr 1(4): 39-46.

Copyright: © 2016 Jiali Xu, et al. This is an open-access article distributed under the terms of the Creative Commons Attribution License, which permits unrestricted use, distribution, and reproduction in any medium, provided the original author and source are credited.

Abstract

This paper deals with a new dynamic decoupling principle, which is a symbiosis of mechanical and control solutions. It is carried out in two steps. At first, the dynamic decoupling of the manipulator involves connecting to initial structure a two-link group forming a Scott-Russell mechanism. The opposite motion of links in the Scott-Russell mechanism combined with optimal redistribution of masses allows the cancellation of the coefficients of nonlinear terms in the manipulator's kinetic and potential energy equations. Then, by using the optimal control design, the dynamic decoupling due to the changing payload is achieved. It becomes relatively easy because in the modified structure of the manipulator with two-link group the coupling and the nonlinearity has been cancelled. The suggested design methodology is illustrated by simulations carried out using ADAMS and MATLAB software, which have confirmed the efficiency of the developed approach.

Keywords: Mechatronic design, Serial manipulators, Decoupled dynamics, Scott-Russell mechanism.

Introduction

Dynamic complexity, such as coupling and nonlinearities is major and it creates problems in the control of manipulator arms. These complex natures of the manipulator dynamics largely come from the payload effect, although they depend upon configuration and operating speed of the manipulator. This problem is critical in robot manipulators designed for high speed applications which have particularly prominent dynamic complexity. The complicated dynamics results from varying inertia, interactions between the different joints, and nonlinear forces such as Coriolis and centrifugal forces. Nonlinear forces cause errors in position response at high speed, and have been shown to be significant even at slow speed [1]. Therefore, in many cases, the reduction (or

cancellation) of coupling and nonlinearity in the manipulators, as it has been shown in [2-5], is necessary.

Feedback linearization is a well-known approach used in controlling such nonlinear systems. The approach involves coming up with a transformation of the nonlinear system into an equivalent linear system through a change of variables and a suitable control input [6-16]. However, it does not guarantee robustness in the face of parameter uncertainty or disturbances such as the payload to be picked up and carried by a robot. Besides that, the permanent tendency to decrease the computing time for the on-line control and as a result computation costs leads to the mechanical solutions permitting the decoupling of dynamic equations by means of an optimal redistribution of moving masses. The developed solutions can be arranged in three principal groups:

a) Decoupling of dynamic equations via actuator relocation. This approach is based on the kinematic decoupling of motions in manipulators when the rotation of any link is due to only one actuator [17-21]. In other terms, it should be assumed that the actuator displacements are a complete set of independent generalized coordinates that are able to locate the manipulator uniquely and completely. The design concept with remote actuation is easy to apply but it is not optimal from point of view of the precise reproduction of the end-effector tasks because it accumulates all errors due to the clearances and elasticity of the belt transmission mainly used in this case. The manufacturing and assembly errors of the added transmission mechanism have also a negative impact to the robot precision.

b) Decoupling of dynamic equations via optimum inertia redistribution [22-27]. In this case, the dynamic decoupling can be achieved when the inertia tensors are diagonal and independent of manipulator configuration. Such an approach

is applied to serial manipulators in which the axis of joints are not parallel. In the case of parallel axes such an approach allows a linearization of dynamic equations but not their dynamic decoupling [28]. Thus, in the case of planar serial manipulators, it cannot be used.

c) Decoupling of dynamic equations via redesign of the manipulator by adding auxiliary links [29-31]. The modification of the manipulator design to achieve high-quality dynamic performance is a new promising tendency in the robotics. However, the design methodology used for such decoupling needs the connection of gears to the oscillating links. The gears added to the oscillating links of the manipulator are sources of shocks between teeth that will lead to the perturbation of the operation of the manipulator, to the noise and other negative effects.

It can therefore be concluded that all known mechanical solutions can only be reached by a considerably more complicated design of the initial structure via adding gears to the oscillating links leading to the revealed drawbacks. The above-mentioned methods provide purely mechanical solutions for dynamic decoupling of motion equations due to the moving masses of manipulator links. However, it is known that the changing payload leads to the perturbation of the dynamic decoupling of the manipulator. Unfortunately, all attempts to carry out a dynamic decoupling of manipulators taking into account the changing payload lead to an unavoidably complicated design. Various actuated counterweights should be applied. Such an approach is not viable.

This paper provides a new decoupling design concept which is a symbiosis of mechanical and control solutions. It is carried out in two steps. At first, the dynamic decoupling of a serial manipulator is achieved via the optimum design of the arm linkage, which consists in the adding of a sub-structure forming with the initial links of the manipulator a Scott-Russell mechanism. Then, the decoupling of dynamic equations is achieved by means of optimal redistribution of moving masses. Such a solution proposed for the first time allows one to carry out the dynamic decoupling without connection of gears to the manipulator links. The elimination of gears from design concept is one of the main advantages of the suggested solution. Thus, the modification of the manipulator structure permits to transform the original nonlinear system model into a fully linear system without using the feedback linearization technique [32]. Then, the dynamic decoupling of motion equations due to the changing payload is carried out via control technique.

It is important to emphasize that the obtained linearized dynamic of the manipulator via adding of a sub-structure, proposed in the present study, leads to the relatively simple equations. Therefore, they are easier to analyze for further dynamic decoupling taking into account the changing payload. In other terms, the proposed mechanical solution leads to the linearized equations of the manipulator, which then facilitate the optimal control design for decoupling of dynamic equations taking into account the changing payload. In this case, there is no need to use the on-line control. This is a second main advantage of the suggested solution.

Such an approach is promising because it combines the advantages of two different principles: mechanical and control.

Conditions of dynamic decoupling via adding a two-link group

Figure 1 shows an improved version of the same arm linkage, which consists of two principal links AB, BP and a sub-group with links BC and CD. The movements of this manipulator are planar motions which are perpendicular to the vertical plane, and therefore, in the present study, not subjected to gravitational forces. The slider D can slide freely along the link AB, and it's connected with link CD by revolute joint D. Thus, the added sub-group with links BC, CD and the slider forms with link BP of the original structure a Scott-Russell mechanism. The Scott Russell mechanism[32] has been invited to generate a theoretically linear motion by using a linkage form with three portions of the links all equal, and a rolling or sliding connection. In this paper, another property of this mechanism is used. The Scott Russell linkage generates also rotations of links by identical angular accelerations, i.e. the angular accelerations of links BC and CD are similar.

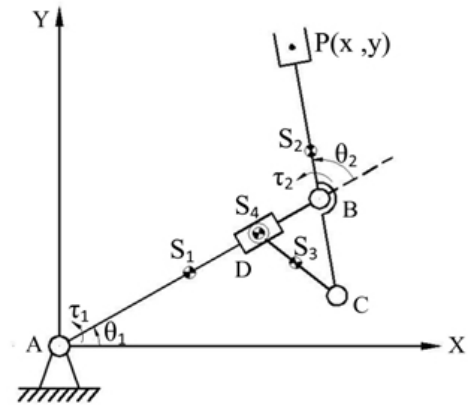


Figure 1: The 2-dof planar serial manipulator with added two-link group

$$\begin{aligned}
 L = & \frac{1}{2} m_1 L_{AS1}^2 \dot{\theta}_1^2 + \frac{1}{2} I_{S1} \dot{\theta}_1^2 + \frac{1}{2} I_{S2} (\dot{\theta}_1 + \dot{\theta}_2)^2 + \frac{1}{2} I_{S3} (\dot{\theta}_1 - \dot{\theta}_2)^2 + \frac{1}{2} I_{S4} \dot{\theta}_1^2 \\
 & + \frac{1}{2} m_2 [L_1^2 \dot{\theta}_1^2 + L_{BS2}^2 (\dot{\theta}_1 + \dot{\theta}_2)^2 + 2L_1 L_{BS2} \cos(\theta_2) \dot{\theta}_1 (\dot{\theta}_1 + \dot{\theta}_2)] \\
 & + \frac{1}{2} m_3 [L_1^2 \dot{\theta}_1^2 + L_3^2 (\dot{\theta}_1 + \dot{\theta}_2)^2 + L_{CS3}^2 (\dot{\theta}_1 - \dot{\theta}_2)^2 - 2L_1 L_3 \cos(\theta_2) \dot{\theta}_1 (\dot{\theta}_1 + \dot{\theta}_2) \\
 & - 2L_1 L_{CS3} \cos(\theta_2) \dot{\theta}_1 (\dot{\theta}_1 - \dot{\theta}_2) + 2L_3 L_{CS3} \cos(2\theta_2) (\dot{\theta}_1^2 - \dot{\theta}_2^2)] \\
 & + \frac{1}{2} m_4 [4L_3^2 \cos^2(\theta_2) \dot{\theta}_1^2 - 4L_1 L_3 \cos(\theta_2) \dot{\theta}_1^2 + L_1^2 \dot{\theta}_1^2 + 4L_3^2 \sin^2(\theta_2) \dot{\theta}_2^2]
 \end{aligned} \quad (1)$$

where, m_1, m_2, m_3, m_4 are the masses of link AB, CP, CD and slider D; $I_{S1}, I_{S2}, I_{S3}, I_{S4}$ are the axial moments of inertia of link AB, CP, CD and slider D; L_1, L_2, L_3 are the lengths of link AB, CP, CD and L_3 also the distance between centers of revolute joints B and C; L_{AS1} is the distance between the center of mass S_1 of link AB and joint center A; L_{BS1} is the distance between the center of mass S_2 of link CP and joint center B; L_{BP} is the distance between the joint center B and the center P of the end-effector; L_{CS3} is the distance between the center of joint C and center of mass of link CD.

Thus, the equations of motion can be written as:

$$\begin{bmatrix} \tau_1 \\ \tau_2 \end{bmatrix} = \begin{bmatrix} D_{11} & D_{12} \\ D_{21} & D_{22} \end{bmatrix} \begin{bmatrix} \ddot{\theta}_1 \\ \ddot{\theta}_2 \end{bmatrix} + \begin{bmatrix} D_{111} & D_{122} \\ D_{211} & D_{222} \end{bmatrix} \begin{bmatrix} \dot{\theta}_1^2 \\ \dot{\theta}_2^2 \end{bmatrix} + \begin{bmatrix} D_{112} & D_{121} \\ D_{212} & D_{221} \end{bmatrix} \begin{bmatrix} \dot{\theta}_1 \dot{\theta}_2 \\ \dot{\theta}_1 \dot{\theta}_2 \end{bmatrix} \quad (2)$$

with

$$\begin{aligned} D_{11} = & m_1 L_{AS1}^2 + I_{S1} + m_2 L_1^2 + m_2 L_{BS2}^2 + 2m_2 L_1 L_{BS2} \cos \theta_2 + I_{S2} + m_3 L_1^2 \\ & + m_3 L_3^2 + m_3 L_{CS3}^2 - 2m_3 L_1 L_3 \cos \theta_2 - 2m_3 L_1 L_{CS3} \cos \theta_2 \\ & + 2m_3 L_3 L_{CS3} \cos(2\theta_2) + I_{S3} + m_4 (2L_3 \cos \theta_2 - L_1)^2 + I_{S4} \end{aligned} \quad (3)$$

$$\begin{aligned} D_{12} = & m_2 L_{BS2}^2 + m_2 L_1 L_{BS2} \cos \theta_2 + I_{S2} + m_3 L_3^2 - m_3 L_{CS3}^2 \\ & - m_3 L_1 L_3 \cos \theta_2 + m_3 L_1 L_{CS3} \cos \theta_2 - I_{S3} \end{aligned} \quad (4)$$

$$\begin{aligned} D_{21} = & m_2 L_{BS2}^2 + m_2 L_1 L_{BS2} \cos \theta_2 + I_{S2} + m_3 L_3^2 - m_3 L_{CS3}^2 \\ & - m_3 L_1 L_3 \cos \theta_2 + m_3 L_1 L_{CS3} \cos \theta_2 - I_{S3} \end{aligned} \quad (5)$$

$$\begin{aligned} D_{22} = & m_2 L_{BS2}^2 + I_{S2} + m_3 L_3^2 + m_3 L_{CS3}^2 - 2m_3 L_3 L_{CS3} \cos(2\theta_2) + I_{S3} \\ & + 4m_4 L_3^2 \sin^2 \theta_2 \end{aligned} \quad (6)$$

$$D_{111} = 0 \quad (7)$$

$$D_{122} = -m_2 L_1 L_{BS2} \sin \theta_2 + m_3 L_1 L_3 \sin \theta_2 - m_3 L_1 L_{CS3} \sin \theta_2 \quad (8)$$

$$\begin{aligned} D_{211} = & m_2 L_1 L_{BS2} \sin \theta_2 - m_3 L_1 L_3 \sin \theta_2 - m_3 L_1 L_{CS3} \sin \theta_2 \\ & + 2m_3 L_3 L_{CS3} \sin(2\theta_2) + 2m_4 L_3 (2L_3 \cos \theta_2 - L_1) \sin \theta_2 \end{aligned} \quad (9)$$

$$D_{222} = 2m_3 L_3 L_{CS3} \sin(2\theta_2) - 2m_4 L_3^2 \sin(2\theta_2) \quad (10)$$

$$\begin{aligned} D_{112} = & -2m_2 L_1 L_{BS2} \sin \theta_2 + 2m_3 L_1 L_3 \sin \theta_2 + 2m_3 L_1 L_{CS3} \sin \theta_2 \\ & - 4m_3 L_3 L_{CS3} \sin(2\theta_2) - 4m_4 L_3 (2L_3 \cos \theta_2 - L_1) \sin \theta_2 \end{aligned} \quad (11)$$

$$D_{121} = D_{212} = D_{221} = 0 \quad (12)$$

where θ_1 is angular displacement of link AB relative to the base; θ_2 is angular displacement of link CP relative to link AB; $\dot{\theta}_1$ is angular velocity of link AB relative to the base; $\dot{\theta}_2$ is angular velocity of link CP relative to link AB; $\ddot{\theta}_1$ is the angular acceleration of link AB relative to the base; $\ddot{\theta}_2$ is the angular acceleration of link CP relative to link AB.

In order to obtain a statically balanced sub-group with links CP and CD, the following conditions must be achieved [34]:

$$\begin{cases} m_3 L_{CS3} + m_4 L_3 = 0 \Rightarrow L_{CS3} = -\frac{m_4}{m_3} L_3 \\ (m_3 + m_4) L_3 - m_2 L_{BS2} = 0 \Rightarrow L_{BS2} = \frac{(m_3 + m_4) L_3}{m_2} \end{cases} \quad (13)$$

then, the equations of the torques can be rewritten as:

$$\begin{cases} \tau_1 = d\ddot{\theta}_1 + b\ddot{\theta}_2 \\ \tau_2 = b\ddot{\theta}_1 + c\ddot{\theta}_2 \end{cases} \quad (14)$$

where

$$\begin{aligned} d = & I_{S1} + I_{S2} + I_{S3} + I_{S4} + m_1 L_{AS1}^2 + (m_2 + m_3 + m_4) L_1^2 \\ & + \left[\frac{(m_3 + m_4)^2}{m_2} + \frac{(m_3 + m_4)^2}{m_3} \right] L_3^2 \end{aligned}$$

$$b = I_{S2} - I_{S3} + \left[\frac{(m_3 + m_4)^2}{m_2} + \frac{m_3^2 - m_4^2}{m_3} \right] L_3^2 \quad (15)$$

$$c = I_{S2} + I_{S3} + \left[\frac{(m_3 + m_4)^2}{m_2} + \frac{(m_3 + m_4)^2}{m_3} \right] L_3^2$$

It is obvious that, if parameter $b = 0$, i.e.

$$I_{S3} = I_{S2} + \left[\frac{(m_3 + m_4)^2}{m_2} + \frac{m_3^2 - m_4^2}{m_3} \right] L_3^2 \quad (16)$$

then the dynamic equations can be completely decoupled. The equations of torques of the manipulator without payload can be written as:

$$\begin{cases} \tau_{1without} = \ddot{\theta}_1 [I_{S1} + 2I_{S2} + I_{S4} + m_1 L_{AS1}^2 + (m_2 + m_3 + m_4) L_1^2 \\ \quad + 2(m_3 + m_4)(m_2 + m_3 + m_4) L_3^2 / m_2] \\ \tau_{2without} = 2\ddot{\theta}_2 [I_{S2} + (m_3 + m_4)(m_2 + m_3 + m_4) L_3^2 / m_2] \end{cases} \quad (17)$$

Thus, the obtained results show that the 2-dof planar serial manipulator with added two-link group forming a Scott-Russell mechanism can be fully dynamically decoupled.

Dynamic decoupling taking into account the payload

The mentioned dynamic decoupling of the equations of motion corresponds to the manipulator without payload. However, the introduction of the changing payload creates the variable loads on the actuators, which are also nonlinear.

First, let us consider the total kinetic energy of the system with payload:

$$\begin{aligned} = & \frac{1}{2} m_1 L_{AS1}^2 \dot{\theta}_1^2 + \frac{1}{2} I_{S1} \dot{\theta}_1^2 + \frac{1}{2} M_2 [L_1^2 \dot{\theta}_1^2 + L_{BS2r}^2 (\dot{\theta}_1 + \dot{\theta}_2)^2] \\ & + 2L_1 L_{BS2r} \cos(\theta_2) \dot{\theta}_1 (\dot{\theta}_1 + \dot{\theta}_2) + \frac{1}{2} I_{S2} (\dot{\theta}_1 + \dot{\theta}_2)^2 + \frac{1}{2} m_3 [L_1^2 \dot{\theta}_1^2 \\ & - L_3^2 (\dot{\theta}_1 + \dot{\theta}_2)^2 + L_{CS3}^2 (\dot{\theta}_1 - \dot{\theta}_2)^2 - 2L_1 L_3 \cos(\theta_2) \dot{\theta}_1 (\dot{\theta}_1 + \dot{\theta}_2) \\ & - 2L_1 L_{CS3} \cos(\theta_2) \dot{\theta}_1 (\dot{\theta}_1 - \dot{\theta}_2) + 2L_3 L_{CS3} \cos(2\theta_2) (\dot{\theta}_1^2 - \dot{\theta}_2^2)] \\ & + \frac{1}{2} I_{S3} (\dot{\theta}_1 - \dot{\theta}_2)^2 + \frac{1}{2} m_4 [4L_3^2 \cos^2(\theta_2) \dot{\theta}_1^2 - 4L_1 L_3 \cos(\theta_2) \dot{\theta}_1^2 \\ & - L_1^2 \dot{\theta}_1^2 + 4L_3^2 \sin^2(\theta_2) \dot{\theta}_2^2] + \frac{1}{2} I_{S4} \dot{\theta}_1^2 \end{aligned}$$

where, $M_2 = m_2 + \Delta_m$, Δ_m is the mass of the payload, and L_{BS2r} is the real distance between the center of mass S_2 of link CP and joint center B, when link CP and the payload were taken as one object.

Then, according to Lagrangian dynamics, the equations of torques of the manipulator with payload can be considered. In this case, the equations of the manipulator balancing can be written as follows [35]:

$$\begin{aligned}
 m_3 L_{CS3} + m_4 L_3 &= 0 \Rightarrow L_{CS3} = -\frac{m_4}{m_3} L_3 \\
 M_2(L_{BP} - L_{BS2r}) &= m_2 \left(L_{BP} - \frac{(m_3 + m_4)L_3}{m_2} \right) \\
 \Rightarrow L_{BS2r} &= \frac{\Delta_m}{M_2} L_{BP} + \frac{(m_3 + m_4)L_3}{M_2}
 \end{aligned} \quad (18)$$

Lastly, together with the condition that described by equation (16), the equations of torques of the manipulator with payload can be written as:

$$\begin{cases}
 \tau_{1with} = \ddot{\theta}_1 [I_{S1} + 2I_{S2} + I_{S4} + m_1 L_{AS1}^2 + (m_2 + m_3 + m_4)L_1^2] \\
 \quad + \ddot{\theta}_1 \left[\frac{2(m_3 + m_4)(m_2 + m_3 + m_4)L_3^2}{m_2} + \Delta_m L_1^2 \right] \\
 \quad + (\ddot{\theta}_1 + \ddot{\theta}_2) \left\{ \frac{[\Delta_m L_{BP} + (m_3 + m_4)L_3]^2}{M_2} - \frac{(m_3 + m_4)^2}{m_2} L_3^2 \right\} \\
 \quad + \ddot{\theta}_1 [2\Delta_m L_1 L_{BP}] \cos \theta_2 + \ddot{\theta}_2 [\Delta_m L_1 L_{BP}] \cos \theta_2 \\
 \quad + \dot{\theta}_1 \dot{\theta}_2 [-2\Delta_m L_1 L_{BP}] \sin \theta_2 + \dot{\theta}_2^2 [-\Delta_m L_1 L_{BP}] \sin \theta_2 \\
 \tau_{2with} = 2\ddot{\theta}_2 [I_{S2} + \frac{(m_3 + m_4)(m_2 + m_3 + m_4)L_3^2}{m_2}] \\
 \quad + (\ddot{\theta}_1 + \ddot{\theta}_2) \left\{ \frac{[\Delta_m L_{BP} + (m_3 + m_4)L_3]^2}{M_2} - \frac{(m_3 + m_4)^2}{m_2} L_3^2 \right\} \\
 \quad + \ddot{\theta}_1 [\Delta_m L_1 L_{BP}] \cos \theta_2 + \dot{\theta}_1^2 [\Delta_m L_1 L_{BP}] \sin \theta_2
 \end{cases} \quad (19)$$

Compared with equations (17), the additional anticipations which are called the payload compensation can be found:

$$\begin{cases}
 \Delta \tau_1 = \ddot{\theta}_1 [\Delta_m L_1^2 + 2\Delta_m L_1 L_{BP} \cos \theta_2] + \ddot{\theta}_2 [\Delta_m L_1 L_{BP} \cos \theta_2] \\
 \quad + (\ddot{\theta}_1 + \ddot{\theta}_2) \left\{ \frac{[\Delta_m L_{BP} + (m_3 + m_4)L_3]^2}{M_2} - \frac{(m_3 + m_4)^2}{m_2} L_3^2 \right\} \\
 \quad + \dot{\theta}_1 \dot{\theta}_2 [-2\Delta_m L_1 L_{BP}] \sin \theta_2 + \dot{\theta}_2^2 [-\Delta_m L_1 L_{BP}] \sin \theta_2 \\
 \Delta \tau_2 = (\ddot{\theta}_1 + \ddot{\theta}_2) \left\{ \frac{[\Delta_m L_{BP} + (m_3 + m_4)L_3]^2}{M_2} - \frac{(m_3 + m_4)^2}{m_2} L_3^2 \right\} \\
 \quad + \ddot{\theta}_1 [\Delta_m L_1 L_{BP}] \cos \theta_2 + \dot{\theta}_1^2 [\Delta_m L_1 L_{BP}] \sin \theta_2
 \end{cases} \quad (20)$$

then, the equations (19) can be rewritten as:

$$\begin{cases}
 \tau_{1with} = \tau_{1without} + \Delta \tau_1 \\
 \tau_{2with} = \tau_{2without} + \Delta \tau_2
 \end{cases} \quad (21)$$

Thus, if the payload compensation that has been shown by equations (20) will be cancelled, the dynamic decoupling of this manipulator with payload can be accomplished. Let us now evaluate the effect of this assumption.

Computer simulation of example study

In order to examine the performance of the proposed approach, the simulations with payload compensation and without payload compensation are performed. And the parameters of the manipulators are the following: $m_1=1.5\text{kg}$, $m_2=1.2\text{kg}$, $m_3=0.5\text{kg}$, $m_4=0.2\text{kg}$, $\Delta_m=1\text{kg}$, $I_{S1}=0.28125\text{kgm}^2$, $I_{S2}=0.144\text{kgm}^2$,

$$I_{S3} = I_{S2} + \left[\frac{(m_3 + m_4)^2}{m_2} + \frac{m_3^2 - m_4^2}{m_3} \right] L_3^2 = 0.47727\text{kgm}^2,$$

$$I_{S4} = 6.6667 \times 10^{-4}\text{kgm}^2, L_1 = 1.5\text{m}, L_2 = 1.2\text{m}, L_3 = 0.5\text{m},$$

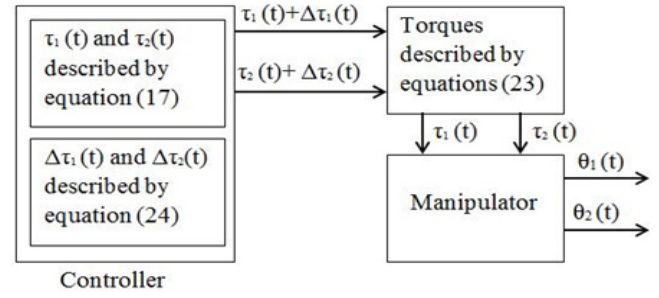


Figure 2: The scheme of the open-loop control system

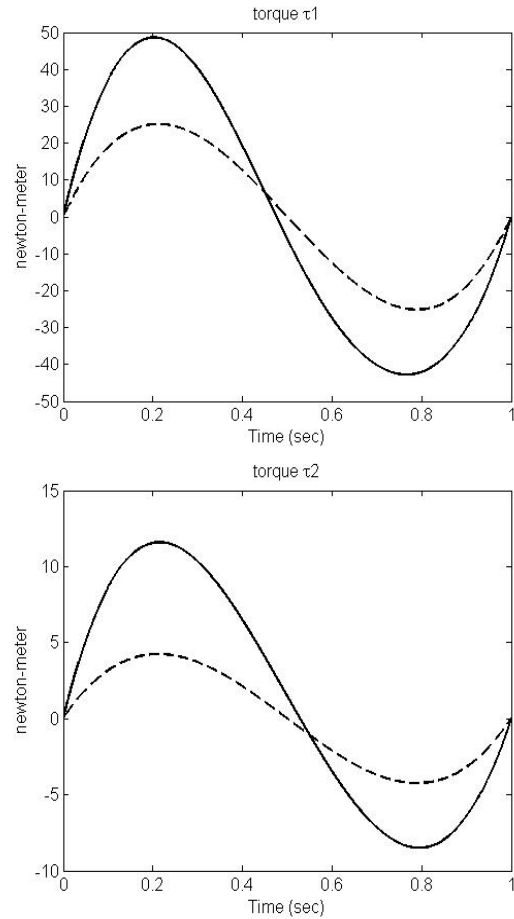


Figure 3: Torques with payload compensation (solid line) and without it (dashed line) for the open-loop system of the model

$$L_{AS1} = 0.75\text{m}, L_{BP} = 0.7\text{m}.$$

The initial and final angles of the actuators are given: $\theta_1^i = 0^\circ$, $\theta_2^i = 30^\circ$, $\theta_1^f = 40^\circ$, $\theta_2^f = 80^\circ$. The generations of motions of the two actuators between the initial and final positions of links 1 and 2 are carried out by fifth order polynomial laws that described as:

$$\begin{cases}
 \theta_{1R}(t) = \theta_1^i + (\theta_1^f - \theta_1^i) \left(\frac{t}{T} \right)^3 \left[10 - 15 \left(\frac{t}{T} \right) + 6 \left(\frac{t}{T} \right)^2 \right] \\
 \theta_{2R}(t) = \theta_2^i + (\theta_2^f - \theta_2^i) \left(\frac{t}{T} \right)^3 \left[10 - 15 \left(\frac{t}{T} \right) + 6 \left(\frac{t}{T} \right)^2 \right]
 \end{cases} \quad (22)$$

where, T is the amount of time taken to execute the proposed trajectories, $0 \leq t \leq T$.

Open-loop control system

The open-loop control law can be written as:

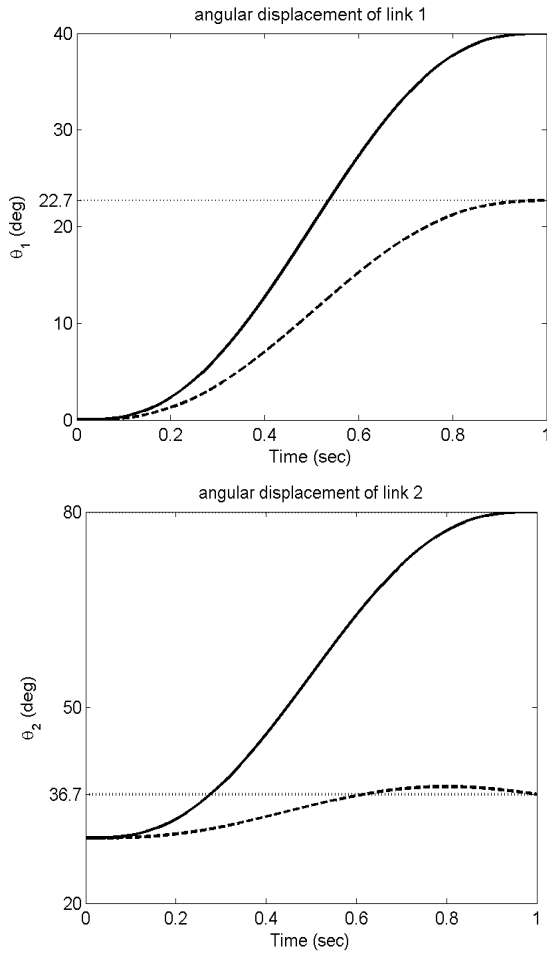


Figure 4: Angular displacements of links AB and BP with payload compensation (solid line) and without it (dashed line) for the open-loop system of the model

$$\begin{cases} \tau_1(t) = d_R \ddot{\theta}_{1R}(t) + \Delta \tau_{1R}(t) \\ \tau_2(t) = c_R \ddot{\theta}_{2R}(t) + \Delta \tau_{2R}(t) \end{cases} \quad (23)$$

where,

$$\begin{aligned} d_R &= I_{S1} + 2I_{S2} + I_{S4} + m_1 L_{AS1}^2 + (m_2 + m_3 + m_4) L_1^2 \\ &\quad + 2(m_3 + m_4)(m_2 + m_3 + m_4) L_3^2 / m_2 \\ c_R &= 2I_{S2} + 2(m_3 + m_4)(m_2 + m_3 + m_4) L_3^2 / m_2 \end{aligned}$$

and the payload compensation is given by:

$$\begin{cases} \Delta \tau_{1R} = \ddot{\theta}_{1R} [\Delta_m L_1^2 + 2\Delta_m L_1 L_{BP} \cos(\theta_{2R})] + \ddot{\theta}_2 [\Delta_m L_1 L_{BP}] \cos(\theta_{2R}) \\ \quad + (\ddot{\theta}_{1R} + \ddot{\theta}_{2R}) \left\{ \frac{[\Delta_m L_{BP} + (m_3 + m_4) L_3]^2}{M_2} - \frac{(m_3 + m_4)^2}{m_2} L_3^2 \right\} \\ \quad + \dot{\theta}_1 \dot{\theta}_2 [-2\Delta_m L_1 L_{BP}] \sin(\theta_{2R}) + \dot{\theta}_{2R}^2 [-\Delta_m L_1 L_{BP}] \sin(\theta_{2R}) \\ \Delta \tau_{2R} = (\ddot{\theta}_{1R} + \ddot{\theta}_{2R}) \left\{ \frac{[\Delta_m L_{BP} + (m_3 + m_4) L_3]^2}{M_2} - \frac{(m_3 + m_4)^2}{m_2} L_3^2 \right\} \\ \quad + \ddot{\theta}_{1R} [\Delta_m L_1 L_{BP}] \cos(\theta_{2R}) + \dot{\theta}_1^2 [\Delta_m L_1 L_{BP}] \sin(\theta_{2R}) \end{cases} \quad (24)$$

First, to demonstrate the influence of the payload compensation, the open-loop control system is executed in MATLAB software, the scheme is shown in Figure 2.

The dashed curves show the torques and the angular displacements

of the manipulator without payload compensation and the solid curves show the same parameters with payload compensation (Figure 3 and 4). It can thus be seen that there are errors between these two cases for tracking the desired trajectories. With payload compensation, both links AB and BP can rotate exactly to the target angles.

But without payload compensation, the errors of angular displacements of link AB and BP are respectively 43.2% and 86.6%. Thus, the effect of feedforward control taking into account the payload is prominent. Thus a feedback control is needed to reduce the influence due to the deletion of the payload compensation.

Closed-loop control system

The closed-loop control law can be written as:

$$\begin{cases} \tau_1(t) = d_R \ddot{\theta}_{1R}(t) + \Delta \tau_{1R}(t) \\ \quad - g_{11} d_R [\dot{\theta}_1(t) - \dot{\theta}_{1R}(t)] - g_{12} d_R [\theta_1(t) - \theta_{1R}(t)] \\ \tau_2(t) = c_R \ddot{\theta}_{2R}(t) + \Delta \tau_{2R}(t) \\ \quad - g_{21} c_R [\dot{\theta}_2(t) - \dot{\theta}_{2R}(t)] - g_{22} c_R [\theta_2(t) - \theta_{2R}(t)] \end{cases} \quad (25)$$

where, $\Delta t_{1R}(t)$ and $\Delta t_{2R}(t)$ are given by the equation (24).

The constant gain elements g_{11} , g_{12} , g_{21} and g_{22} are obtained by an optimal poleplacement design through state feedback. The state space representation of the manipulator, which is statically balanced, will be written as:

$$\begin{bmatrix} \dot{\theta}_1(t) \\ \dot{\theta}_1(t) \\ \dot{\theta}_2(t) \\ \dot{\theta}_2(t) \end{bmatrix} = \underbrace{\begin{bmatrix} 0 & 1 & 0 & 0 \\ 0 & 0 & 0 & 0 \\ 0 & 0 & 1 & 0 \\ 0 & 0 & 0 & 0 \end{bmatrix}}_A \begin{bmatrix} \theta_1 \\ \dot{\theta}_1 \\ \theta_2 \\ \dot{\theta}_2 \end{bmatrix} + \underbrace{\begin{bmatrix} 0 & 0 \\ \frac{1}{d} & 0 \\ 0 & 0 \\ 0 & \frac{1}{c} \end{bmatrix}}_B \begin{bmatrix} \tau_1(t) \\ \tau_2(t) \end{bmatrix} \quad (26)$$

The controllable canonical form is given by two independent subsystems as follows:

$$\begin{cases} \begin{bmatrix} d \ddot{\theta}_1 \\ d \dot{\theta}_1 \end{bmatrix} = \begin{bmatrix} 0 & 0 \\ 1 & 0 \end{bmatrix} \begin{bmatrix} d \dot{\theta}_1 \\ d \theta_1 \end{bmatrix} + \begin{bmatrix} 1 \\ 0 \end{bmatrix} \tau_1(t) \\ \begin{bmatrix} c \ddot{\theta}_2 \\ c \dot{\theta}_2 \end{bmatrix} = \begin{bmatrix} 0 & 0 \\ 1 & 0 \end{bmatrix} \begin{bmatrix} c \dot{\theta}_2 \\ c \theta_2 \end{bmatrix} + \begin{bmatrix} 1 \\ 0 \end{bmatrix} \tau_2(t) \end{cases} \quad (27)$$

A double integrator

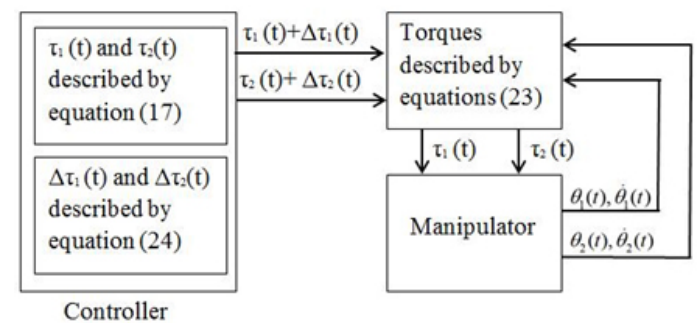


Figure 5: The scheme of the closed-loop system

$$\begin{bmatrix} \ddot{\varphi}(t) \\ \dot{\varphi}(t) \end{bmatrix} = \underbrace{\begin{bmatrix} 0 & 0 \\ 1 & 0 \end{bmatrix}}_A \underbrace{\begin{bmatrix} \dot{\varphi}(t) \\ \varphi(t) \end{bmatrix}}_{x(t)} + \underbrace{\begin{bmatrix} 1 \\ 0 \end{bmatrix}}_B u(t)$$

is completely controllable. We seek $u(t)$ that minimize the cost

$$J = \int_0^{\infty} [x^T(t) Q x(t) + \tau^2(t)] dt$$

where the matrix Q is based on the controllability grammien defined by:

$$G_c(0, T_p) = \int_0^{T_p} [e^{At} B B^T e^{A^T t}] dt \quad (28)$$

The matrix $Q = [T_p G_c(0, T_p)]^{-1}$ is symmetric and positive definite. The parameter T_p assume that poles of closed-loop system may be placed, in the S plane, at the left of the vertical straight with the abscissa $-\frac{1}{T_p}$.

The linear quadratic controller is unique, optimal

$u(t) = -G x(t)$, full state feedback controll law with $G = B^T \Sigma$ that minimized the cost J .

The matrix Σ is the unique, symmetric, positive definite solution

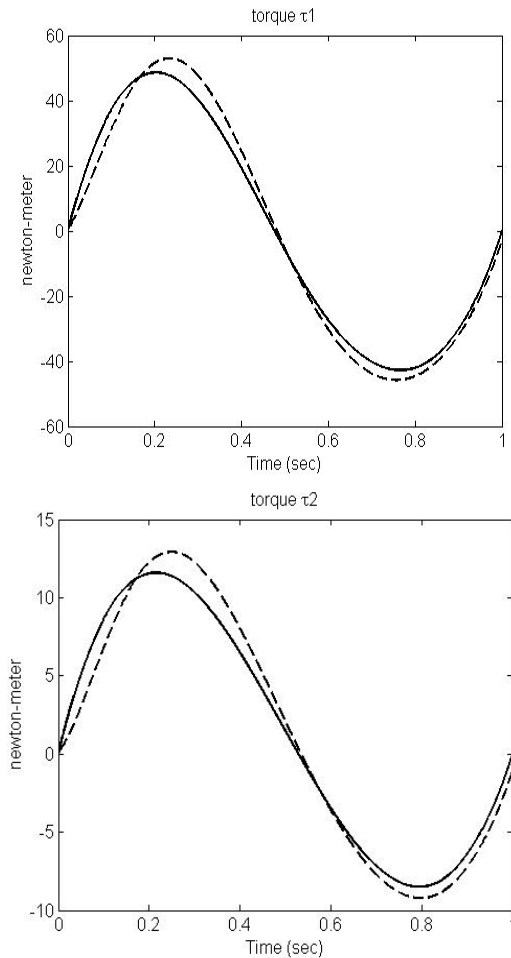


Figure 6: Torques with payload compensation (solid line) and without it (dashed line) for the closed-loop system of the model

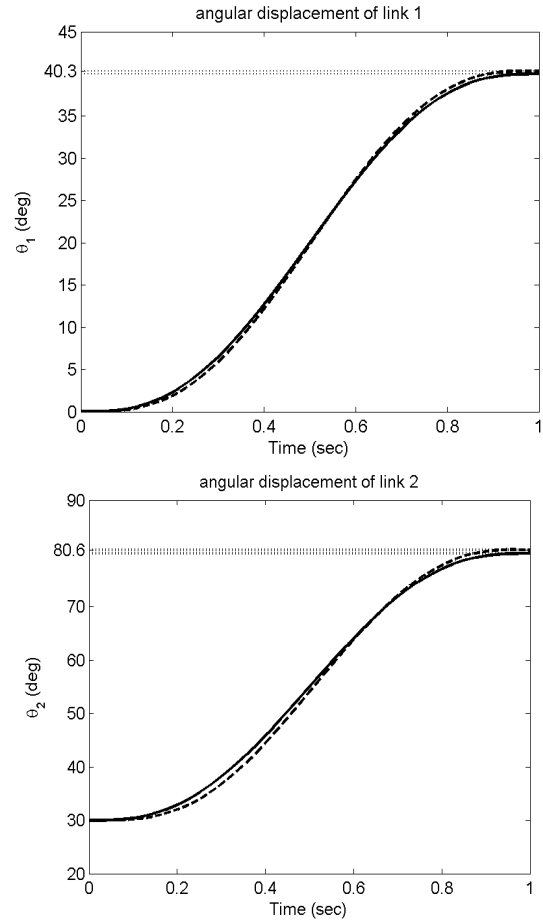


Figure 7: Angular displacements of links AB and BP with payload compensation (solid line) and without it (dashed line) for the closed-loop system of the model

to the algeric Riccati equation: $A^T \Sigma + \Sigma A - \Sigma B B^T \Sigma + Q = 0$. As a result,

$$g_{11} = g_{12} = \frac{2\sqrt{1+\sqrt{3}}}{T_p}, g_{21} = g_{22} = \frac{2\sqrt{3}}{T_p^2}$$

Then the closed-loop characteristic polynomial is:

$$P(s) = s^2 + \frac{2\sqrt{1+\sqrt{3}}}{T_p} s + \frac{2\sqrt{3}}{T_p^2}$$

If $P(s) = s^2 + 2\zeta\omega_n s + \omega_n^2$, then $\omega_n = \frac{\sqrt{2\sqrt{3}}}{T_p}$ and $\zeta = \frac{\sqrt{1+\sqrt{3}}}{\sqrt{2\sqrt{3}}}$.

For $T = 1s$, $T_p = 0.1s$ and $\Delta_m = 1kg$, the scheme of the closed-loop system in the MATLAB software is shown in Figure 5 and the simulation results are presented at Figure 6 and 7.

As in the simulation of open-loop system, the dashed curves show the torques and the angular displacements of the manipulator without payload compensation and the solid curves show the same parameters with payload compensation (Figure6 and 7).

Like in previous simulations, the payload compensation allows an exact reproduction of manipulator motions. However, with the feedback control, the errors of angular displacements of link AB and BP with payload compensation and without it (Figure7)

are 0.73% and 1.23% respectively. Thus the use of the feedback reduces prominently the errors.

Discussion

As mentioned above, the dynamic decoupling can eliminate the effect of the complicated dynamics results from varying inertia, interactions between the different joints, and nonlinear forces such as Coriolis and centrifugal forces. It has been shown that the tracking accuracy of the manipulator can be improved. To illustrate the advantages of the proposed solution, additional simulations of the initial structure of a 2-dof planar serial manipulator were performed. Focusing on the simulation results under the closed-loop system, for the initial structure, the positioning errors of the two actuated links AB and BP were 0.199% and 2.29%, respectively. These results have been obtained for simulations without payload. Then, the simulations with payload of 1 kg were performed. In this case, the positioning errors of the two actuated links AB and BP have been increased to 1.23% and 11.6%, respectively. So, these simulations showed that the proposed dynamic decoupling solution ensures a significant improvement in tracking accuracy.

Conclusion

This paper deals with a new dynamic decoupling principle, which is a symbiosis of mechanical and control solutions. It is carried out in two steps.

At first, the dynamic decoupling of the serial manipulator is accomplished via the Scott-Russell mechanism properties and optimal redistribution of masses. Thus, the modification of the mass redistribution allows one to transform the original nonlinear system model into a fully linear system without using the feedback linearization technique. Such a solution of the dynamic decoupling of motion equations via adding a two-link group and forming with initial structure a Scott-Russell mechanism is proposed for the first time. It allows one to carry out the dynamic decoupling without connection of gears to the manipulator links. The elimination of gears from design concept is one of the main advantages of the suggested mechanical solution. However, it is obvious that the changing payload leads to the perturbation of the dynamic decoupling of the manipulator. To ensure linearized and decoupled dynamics of the manipulator for any payload, an optimal control technique is applied. It should be emphasized that the proposed mechanical solution leads to the linearized equations of the manipulator, which then facilitate the optimal control design for decoupling of dynamic equations taking into account the changing payload. In this case, there is no need to use the on-line control. This is a second main advantage of the suggested solution.

Simulations of the proposed structure in the case of the open-loop system, as well as the closed-loop system are performed. The numerical simulations with the feedback control show that the errors of angular displacements of the actuated links with payload compensation and without it are 0.73% and 1.23% respectively.

In order to illustrate the advantage of the suggested dynamic decoupling solution, the same simulations of a 2-dof planar serial manipulator with added two-link group and without it are also performed. According to the comparison between the simulation results of these two structures, it is revealed that the proposed

dynamic decoupling solution ensures a significant improvement in tracking accuracy.

References

1. Brady M. Robot Motion: Planning and Control. MIT Press. 1982.
2. Herman P. Energy based indexes for manipulator dynamics improvement. *Journal of Intelligent and Robotic Systems*. 2005; 44:313–325.
3. Herman P. Non-linearity evaluation and reduction for serial manipulators. In: *Proceedings of the Institution of Mechanical Engineers: Journal of Multibody Dynamics – Part K*. 2006; 220:283–291.
4. Pons JL, Ceres R, Jimenez AR, Calderon L, Martin JM. Nonlinear performance index: a tool for manipulator dynamics improvement. *Journal of Intelligent and Robotic Systems*. 1997; 18:277–87.
5. Herman P. Dynamical couplings reduction for rigid manipulators using generalized velocity components. *Mechanics Research Communications*. 2008; 35:553–561.
6. Vukobratovic M, Potkonjak V. *Dynamics of Manipulation Robots: Theory and Application*. Berlin: Springer Verlag; 1982.
7. Vukobratovic M, Stokic D, Kircanski N. *Nonadaptive and Adaptive Control of Manipulation Robots*. Berlin: Springer Verlag; 1985.
8. Sciacivco L, Siciliano B. *Modelling and Control of Robot Manipulators*. New York: The McGraw-Hill Companies; 1996.
9. Slotine JJ, Li W. *Applied Nonlinear Control*. New Jersey: Prentice Hall; 1991.
10. Kim HS, Cho YM, Lee K. Robust nonlinear task space control for a 6 DOF parallel manipulator. *Automatica*. 2005; 41:1591–600.
11. Ting Y, Chen YS, Jar HC. Modelling and control for a Gough–Stewart platform CNC machine. *Journal of Robotics System*. 2004; 21:609–623.
12. Chen JL, Chang WD. Feedback linearization control of a two-link robot using a multi-crossover genetic algorithm. *Expert Systems with Applications*. 2009; 36:4154–4159.
13. Duchaine V, Bouchard S, Gosselin CM. Computationally efficient predictive robot control. *IEEE/ASME Transactions on Mechatronics*. 2007; 12:570–578.
14. Davliakos E, Papadopoulos, Model-based control of a 6-DOF electrohydraulic Stewart–Gough platform. *Mechanism and Machine Theory*. 2008; 43:1385–1400.
15. Chen YX, McInroy JE. Decoupled control of flexure-jointed hexapods using estimated joint-space mass–inertia matrix. *IEEE Transactions on Control Systems Technology*. 2004; 12:413–421.
16. Yang C, Huang Q, Han J. Decoupling control for spatial six-degree-of-freedom electro-hydraulic parallel robot. *Robotics and Computer-Integrated Manufacturing*. 2012; 28:14–23.
17. Asada H, Youcef-Toumi K. *Direct-Drive Robots*. MIT Press; 1986.
18. Korendyasev AL, et al. *Manipulation systems of robots*. Moscow: Mashinostroyeniya; 1989.
19. Minotti P. Découplage dynamique des manipulateurs: propositions de solutions mécaniques. *Mechanism and Machine Theory*. 1991; 26(1):107–122.
20. Vukobratovic KM, Stokic DM. Contribution to the decoupled control of large-scale mechanisms. *J. Automatica*. 1980; 16:9–21.
21. Young-Hoon Chug, Jeong-Gun Gang, Jae-Won Lee. The Effect of Actuator Relocation on Singularity, Jacobian and Kinematic Isotropy of Parallel Robots. In: *Proceedings of the 2002 IEEE WRSJ Intl. Conference on Intelligent Robots and Systems EPFL*. 2002 Oct. Lausanne, Switzerland. p. 2147–2153.

22. Asada H, Slotine JJE. *Robot Analysis and Control*. John Wiley and Sons; 1986.
23. Yang DCH, Tzeng SW. Simplification and linearization of manipulator dynamics by design. In: *Proceedings of the 9th Applied Mechanics Conference*. 1985 Oct. Kansas City, Missouri. p. 28–30.
24. Yang DCH, Tzeng SW. Simplification and linearization of manipulator dynamics by the design of inertia distribution. *The International Journal of Robotics Research*. 1986; 5(3):120–128.
25. Abdel-Rahman TM, Elbestawi MA. Synthesis and dynamics of statically balanced direct-drive manipulators with decoupled inertia tensors. *Mechanism and Machine Theory*. 1991; 26(4):389–402.
26. Minotti P, Pracht P. Design of robots driven by linear servo systems. *Robotica*. 1992; 10:361–368.
27. Filaretov VF, Vukobratovic MK. Static balancing and dynamic decoupling of the motion of manipulation robots. *Mechatronics*. 1993; 3(6):767–82.
28. Rompertz RS, Yang DCH. Performance evaluation of dynamically linearized and kinematically redundant planar manipulators. *J. Robotic & Computer Integrated Manufacturing*. 1989; 5(4):321-331.
29. Coelho T, Yong L, Alves V. Decoupling of dynamic equations by means of adaptive balancing of 2-dof open-loop mechanisms. *J. Mechanism and Machine Theory*. 2004; 39(8):871-81.
30. Moradi M, Nikoobin A, Azadi S. Adaptive decoupling for open chain planar robots. *J. Scientia Iranica: Transaction B, Mechanical Engineering*. 2010; 17(5):376-86.
31. Arakelian V, Sargsyan S. On the design of serial manipulators with decoupled dynamics. *J. Mechatronics*. 2012; 22(6):904-909.
32. Arakelian V, Le Baron JP, Mottu P. Torque minimization of the 2-DOF serial manipulators based on minimum energy consideration and optimum mass redistribution. *Mechatronics*. 2011; 218:310-314.
33. Freemantle W. Straight-line linkage. British Patent 2741. 1803 Nov 17.
34. Briot S, Bonev I, Gosselin C, Arakelian V. Complete Shaking Force and Shaking Moment Balancing of Planar Parallel Manipulators with Prismatic Pairs. *J. Multi-body Dynamics*. 2009; 223:43-52.
35. Arakelian V, Briot S. Balancing of linkages and robot manipulators. *Advanced methods with illustrative examples*. Springer; 2015.